

1

2 **Pathophysiological Analysis of the Progression of Hepatic Lesions in**
3 **STAM Mice**

4

5 **T. SAITO¹, M. MURAMATSU¹, Y. ISHII¹, Y. SAIGO¹, T. KONUMA¹, Y.**
6 **TORINIWA¹, K. MIYAJIMA², T. OHTA¹**

7

8 ¹Biological/Pharmacological Research Laboratories, Central Pharmaceutical Research
9 Institute, Japan Tobacco Inc., 1-1 Murasaki-cho, Takatsuki, Osaka 569-1125, Japan

10 ²Toxicology Research Laboratories, Central Pharmaceutical Research Institute, Japan
11 Tobacco Inc., 23 Naganuki, Hadano, Kanagawa 257-0024, Japan

12

13 **Corresponding author**

14 T. Ohta, Biological/Pharmacological Research Laboratories, Central Pharmaceutical
15 Research Institute, Japan Tobacco Inc., 1-1 Murasaki-cho, Takatsuki, Osaka 569-1125,
16 Japan, E-mail: takeshi.ota@jt.com

17

18 **Short title**

19 Hepatic Lesions in STAM Mice

20

21

1 **Summary**

2 Nonalcoholic steatohepatitis (NASH) is a current health issue since the disease often
3 leads to hepatocellular carcinoma; however, the pathogenesis of the disease has still not
4 been fully elucidated. In this study, we investigated the pathophysiological changes
5 observed in hepatic lesions in STAM mice, a novel NASH model. STAM mice, high
6 fat-diet (HFD) fed mice, and streptozotocin (STZ) treated mice were prepared, and
7 changes over time, such as biological parameters, mRNA expression, and
8 histopathological findings, were evaluated once animal reached 5, 7, and 10 weeks of
9 age. STZ mice presented with hyperglycemia and an increase in oxidative stress in
10 immunohistochemical analyses of Hexanoyl-lysine: HEL from 5 weeks, with fibrosis in
11 the liver also being observed from 5 weeks. HFD mice presented with hyperinsulinemia
12 from 7 weeks and the slight hepatosteatosis was observed at 5 weeks, with changes
13 significantly increasing until 10 weeks. STAM mice at 10 weeks showed significant
14 hepatic changes, including hepatosteatosis, hypertrophic hepatocytes, and fibrosis,
15 indicating pathological changes associated with NASH. These results suggested that the
16 increase in oxidative stress with hyperglycemia triggered hepatic lesions in STAM mice,
17 and insulin resistance promoted lesion formation with hepatic lipid accumulation.
18 STAM mice may be a useful model for elucidating the pathogenesis of NASH with
19 diabetes.

20 **Key words**

1 Diabetes·NASH·STAM mice

2

1 **Introduction**

2 Nonalcoholic fatty liver disease (NAFLD) is presently recognized as the most
3 common chronic liver disease and a major hepatic health issue in the world (Clark,
4 2006; de Alwis and Day, 2008; Zelber-Sagi et al., 2006). NAFLD is associated with
5 obesity, diabetes, insulin resistance, dyslipidemia, and hypertension (de Alwis and Day,
6 2008; Falck-Ytter et al., 2001).

7 NAFLD presents with fatty liver pathology, including simple steatosis, nonalcoholic
8 steatohepatitis (NASH), and cirrhosis, with 4-22% of NAFLD patients developing
9 hepatocellular carcinoma (Ertle et al., 2011; Greenfield et al., 2008). However, the
10 pathogenesis of NAFLD and the progression to fibrosis and chronic liver disease
11 remains poorly defined, and effective pharmacological therapies, in particular for
12 NASH, have not been approved. The leading hypothesis for this liver disease is the
13 two-hit model (Day and James, 1998). The first hit is initial metabolic changes, such as
14 hyperglycemia, insulin resistance, hyperlipidemia, and lipid accumulation in the liver,
15 leading to steatosis. The second hit including genetic and environmental factors triggers
16 the progression to more severe liver pathologies.

17 To elucidate the complicated features of NAFLD/NASH, animal models offer
18 important information. As NAFLD/NASH animal models, ob/ob mice, db/db mice,
19 KK-Ay mice, Zucker fatty (ZF) rats, and Spontaneously Diabetic Torii (SDT) fatty rats
20 develop spontaneous hepatic steatosis based on insulin resistance and obesity (Ishii et

1 al., 2015; Kucera and Cervinkova, 2014; Takahashi et al., 2012). Moreover, dietary
2 models, such as high fat- and fructose-fed models, are well known as NAFLD/NASH
3 models (Takahashi et al., 2012). Recently, a NASH-derived hepatocellular carcinoma
4 (HCC) model (STAM model) was reported by Fujii *et al.* (Fujii et al., 2013). The
5 STAM model fulfills criteria for HCC diagnoses and demonstrates the following
6 features: having at least 4 detectable tumor nodules, an average tumor growth rate of
7 150% from 16 to 20 weeks of age, no visible metastases, and relatively preserved liver
8 function (Takakura et al., 2014).

9 In this study, we investigated the pathophysiological changes observed in hepatic
10 lesions during the early stages in STAM mice by comparing this model with mice fed a
11 high fat diet and/or treated with streptozotocin (STZ).

12

13 **Materials and Methods**

14

15 *Animals and chemicals*

16 This experiment was conducted in compliance with the Guidelines for Animal
17 Experimentation at biological/pharmacological research laboratories of Japan Tobacco.
18 Pathogen-free pregnant C57BL/6J mice (CLEA Japan, Tokyo, Japan) at 14 days of age
19 were purchased, and male pups were used in this study. Four groups: the STAM group,
20 high fat diet-fed (HFD) group, STZ-treated (STZ) group, and normal group, were

1 prepared.

2 Hepatic lesions in the STAM group were induced by a single subcutaneous injection
3 of 200 µg of STZ (Sigma, MO, USA) 2 days after birth followed by feeding with a 32%
4 fat high-fat diet (HFD32; CLEA Japan, Tokyo, Japan) *ad libitum* after 4 weeks of age.
5 Mice in the HFD group were fed the high-fat diet (HFD32) after 4 weeks of age. In
6 mice in the STZ group, a single subcutaneous injection of 200 µg of STZ was
7 administered 2 days after birth. Mice in the normal group were fed a standard diet
8 (CRF-1, Charles River Japan, Yokohama, Japan). The mice were housed in a
9 climate-controlled room with a temperature of $23 \pm 3^\circ\text{C}$, humidity $55 \pm 15\%$, and a 12-h
10 dark-light cycle.

11

12 *Biochemical parameters*

13 Body weight and biochemistry parameters in the blood were monitored at 5, 7, and 10
14 weeks of age. Blood samples were collected from the orbital venous plexus under
15 non-fasting conditions. Glucose, triglycerides (TG), total cholesterol (TC), alanine
16 aminotransferase (ALT), and aspartate aminotransferase (AST) levels were measured
17 using commercial kits (Roche Diagnostics, Basel, Switzerland) and an automatic
18 analyzer (Hitachi 7180; Hitachi High-Technologies, Tokyo, Japan). Commercial ELISA
19 kits were used to measure serum insulin (Rat Insulin ELISA Kit; Morinaga Institute of
20 Biological Science, Yokohama, Japan).

1

2 *Tissue sampling and histopathology*

3 Necropsy was performed at 5, 7, and 10 weeks of age. All animals were sacrificed by
4 exsanguination under isoflurane anesthesia. The livers were sampled for gene
5 expression, hepatic lipid content, and histopathological analysis. Samples for gene
6 expression and hepatic lipid content analyses were stored at -80°C until testing. For
7 histopathological examinations, the livers were immediately fixed in 10% formalin
8 neutral buffer solution (v/v, formaldehyde:1, phosphate buffer:9, pH7.4). After resection,
9 the tissues were paraffin-embedded using standard techniques and thin-sectioned (3 to 5
10 µm). The sections were stained with hematoxylin and eosin (HE) and Sirius Red. These
11 samples were all examined histopathologically, and findings were graded from normal
12 (-) to severe (+++). Immunohistochemical analysis of hexanoyl-lysine (HEL) regarding
13 the oxidative stress, malignancy and fibrosis were performed in the liver section from 5
14 weeks of age in all groups. Staining was visualized using DAB Peroxidase Substrate kit
15 (JalCA, Sizuoka, Japan) to produce a brown reaction product indicating antigen
16 localization. Anti-mouse Hexanoyl-Lysine adduct (HEL, JalCA, Sizuoka, Japan) was
17 used for immunochemical detection of hepatocyte in liver.

18

19 *Hepatic TG and TC content*

20 A portion of the liver weighing approximately 100 mg, 0.5 mL of methanol, and

1 zirconia beads were added to tubes. The liver portion was homogenized using a mixer
2 mill (MM300 Retch) (25 Hz, 10 min). To the homogenized solution, 1 mL of
3 chloroform was added and mixed thoroughly. The mixture was then centrifuged (10,000
4 g, 5 min, 4C°) and the resulting supernatant collected. Solvents contained in 0.5 mL of
5 the supernatant were dried under a stream of nitrogen gas. To the residue, 0.5 mL of
6 2-propanol was added, and the residue was subsequently dissolved again. TG and TC
7 concentrations in the 2-propanol solution were determined using the biochemistry
8 automatic analyzer (Hitachi 7170S; Hitachi, Tokyo, Japan).

9

10 *mRNA quantification with real-time quantitative PCR*

11 Total RNA was extracted from the livers of animals at 5, 7, and 10 weeks of age.
12 RNA was transcribed into cDNA using M-MLV reverse transcriptase and random
13 primers (Invitrogen, Carlsbad, CA). The reaction mixture was incubated for 10 min at
14 25°C, 1 h at 37°C, and 5 min at 95°C. Real-time PCR quantification was performed in a
15 50-μL reaction mixture with an automated sequence detector combined with ABI Prism
16 7700 Sequence Detection System software (Applied Biosystems, Foster City, CA). The
17 reaction mixture contained 50 ng of synthesized cDNA, 3.5 mM MgCl₂, 0.3 μM
18 primers, 0.1 μM probes, and 1.25 units of Ampli Taq Gold®. Cycle parameters were 10
19 min at 95°C, followed by 40 cycles of 15 s at 95°C and 60 s at 60°C. The following
20 primer and FAM-conjugated probe were designed using Primer Express software

1 (Applied Biosystems): Tumor Necrosis Factor (TNF) α (forward,
2 AGACCCTCACACTCAGATCATCTTC; reverse, ACTTGGTGGTTTGCTACGACG;
3 probe, CAAAATTCGAGTGACAAGCCTGTAGCCC), and β -actin (purchased from
4 Applied Biosystems). The expression of Tissue Inhibitor of Metalloproteinase (TIMP) 1
5 (Mm0041818_m1) was confirmed using Taqman Gene Expression Assays.

6

7 *Statistical analysis*

8 The results of biological parameters are expressed as the mean \pm standard
9 deviation (SD). Statistical analyses of differences between mean values were performed
10 using a Tukey Kramer test. Differences were considered significant at $p < 0.05$.

11

12 **Results**

13

14 The STAM group showed decreases in body weight and blood insulin levels in
15 comparison with the normal group, and mice in the HFD group showed obesity and
16 hyperinsulinemia in comparison with the STAM group during the experimental period
17 (Body weight at 10 weeks of age: HFD, 37.5 ± 3.5 g vs. STAM, 21.1 ± 1.9 g, Blood
18 insulin level at 10 weeks of age: HFD, 2.54 ± 0.86 ng/ml vs. STAM, 0.33 ± 0.13 ng/ml)
19 (Figs. 1A and 1C). Mice in both the STAM and STZ groups showed significant
20 hyperglycemia from 5 weeks of age (STAM, 594.3 ± 108.3 mg/dl, STZ, 472.5 ± 126.3

1 mg/dl, HFD, 253.5 ± 15.0 mg/dl), and the hyperglycemia was sustained during the
2 experimental period (Fig. 1B). Blood TG and TC levels in the STZ group gradually
3 increased in comparison with the normal group during the experimental period. Blood
4 TC levels in the HFD group also increased over time; however, TG levels did not
5 change in comparison with the normal group during the experimental period (Figs. 1D
6 and 1E). Blood ALT levels in the STAM and STZ groups significantly increased at 5 or
7 7 weeks of age in comparison with the normal group, and the level in the HFD group
8 tended to increase, although this increase was not significant (Fig. 1F). Changes in
9 blood AST levels followed a similar pattern as blood ALT levels (data not shown).

10 Relative liver weights in the STAM group showed significant increases during the
11 experimental period, and the weights in the STZ group showed significant increases at 7
12 and 10 weeks of age in comparison with the normal group; however, the weights in the
13 HFD group did not show increases in comparison with the normal group (Fig. 2A).
14 Hepatic TG content in the STAM and HFD groups showed significant increases in
15 comparison with the normal group during the experimental period, and TC content also
16 showed an increase or a tendency to increase (Figs. 2B and 2C). Mice in the STZ group
17 did not show significant increases in hepatic lipid content. Changes in the mRNA
18 expression of $\text{TNF}\alpha$, an inflammation related factor, and TIMP1, a fibrosis related
19 factor, were determined for each group (Figs. 2D and 2E). Both $\text{TNF}\alpha$ and TIMP1
20 mRNA expression in the HFD and STZ groups showed a tendency to increase in

1 comparison with the normal group; however, the changes were not significant. TNF α
2 and TIMP1 mRNA expression in the STAM group also showed a tendency to increase
3 in comparison with the normal group, and TNF α expression at 10 weeks of age
4 significantly increased in comparison with the normal group (Fig. 2D).

5 Liver histopathologies were examined by HE staining, and Sirius Red staining to
6 evaluate fibrosis (Table 1, Figs. 3 and 4). In STAM mice, moderate or severe changes in
7 hepatosteatosis were observed from 5 weeks of age, and moderate or severe changes in
8 hypertrophic hepatocytes from 7 weeks of age and significant changes in fibrosis were
9 observed until 10 weeks of age. In mice in the HFD group, slight hepatosteatosis was
10 observed from 5 weeks of age, and moderate or severe changes in hypertrophic
11 hepatocytes were observed at 10 weeks of age. Moreover, the fibrosis in the HFD group
12 was observed from 7 weeks of age. In mice in the STZ group, the hepatic fibrosis was
13 observed from 5 weeks of age (6 rats in 8 rats), and very slight changes in
14 hepatosteatosis and hypertrophic hepatocytes were observed at 10 weeks of age. In
15 immunohistochemical examinations, HEL, an indicator of oxidative DNA damage,
16 positive cells were detected in tissues of the STZ group, but not detected in the normal
17 group (Figs. 3I-3L).

18

19 **Discussion**

20

1 Recently, the incidence of NAFLD has increased worldwide with the increased
2 prevalence of obesity, type 2 diabetes, and dyslipidemia, and approximately 10% of
3 NAFLD patients develop NASH, in which hepatic steatosis is related to inflammation
4 and hepatocyte apoptosis (Bugianesi et al., 2002; Clark, 2006; Day and James, 1998).
5 Furthermore, NASH leads to fibrosis, liver cirrhosis, and eventually hepatocellular
6 carcinoma. According to the two-hit hypothesis for NASH progression, the first hit is
7 lipid accumulation in hepatocytes via metabolic disorders, and the second hit is a
8 combination of multiple factors, including genetics, insulin resistance, oxidative stress,
9 and inflammation (Day and James, 1998; Dowman et al., 2010). However, the precise
10 mechanism for the progression from hepatic steatosis to NASH has yet to be elucidated.

11 Several animal models have been developed to understand the pathogenesis of
12 NAFLD/NASH. The STAM model is the first animal model that is a NASH-derived
13 HCC model expected to establish pharmacological intervention against HCC (Fujii et al.,
14 2013; Takakura et al., 2014). HCC in the STAM model is reportedly equivalent to
15 stages B to C disease classified in accordance with the Barcelona Clinic Liver Cancer
16 staging system for humans (Takakura et al., 2014). We investigated the
17 pathophysiological features of early hepatic lesions, from hepatic steatosis to fibrosis,
18 by comparing the onset of lesions and progression among three groups, the STAM
19 group, HFD group, and STZ group.

20 In comparison of histopathological findings in livers among three groups,

1 hepatosteatosis, hypertrophy hepatocyte, and fibrosis were observed from 5 weeks of
2 age in the STAM group; however, the fibrosis was not observed at 5 weeks of age in the
3 HFD group. On the other hand, the fibrosis was observed from 5 weeks of age in the
4 STZ group with the increase of blood glucose level. Moreover, the changes of
5 hepatosteatosis and hypertrophy hepatocyte in the HFD group were enhanced
6 periodically from 5 to 10 weeks of age; however those changes in the STZ group were
7 very slight at 10 weeks of age.

8 In this study, the STAM group showed hepatic lesions, such as hepatosteatosis,
9 hypertrophic hepatocytes, and fibrosis, as previously reported. STZ group showed
10 significant hyperglycemia and hepatic fibrosis at 5 weeks of age; however, the HFD
11 group did not show fibrosis at 5 weeks of age. Moreover, the oxidative stress marker of
12 HEL was detected in the hepatocytes of animals in the STZ group, and
13 inflammation-related mRNA also tended to increase at 5 weeks of age. Initial hepatic
14 lesions, including fibrosis, in STAM mice are considered to be caused by oxidative
15 stress with sustained hyperglycemia. Chronic hyperglycemia reportedly leads to the
16 production of reactive oxygen species (ROS) and oxidative stress. Hyperglycemia
17 induces the overproduction of NADH and mitochondrial ROS that inhibit
18 glyceraldehyde 3-phosphate dehydrogenase (GAPDH) activity (Giacco and Brownlee,
19 2010; Paradies et al., 2014; Yan, 2014). The oxidative stress is considered to be an
20 important factor in causing lethal hepatocyte injury associated with NAFLD/NASH.

1 ALT levels at 5 weeks of age in the STZ group tended to increase, and the inflammation
2 may be induced by oxidative stress. The increase of TIMP1 may also be associated with
3 the development of hepatic fibrosis. High glucose reportedly increases the expression of
4 mRNA and protein of matrix metalloproteinase 1 (MMP1) (Yang et al., 2009). Overt
5 hyperglycemia was observed at 10 weeks of age in the STZ group. Carbohydrate
6 content in the diet (crude fat, 32% and nitrogen free extracts, 29.4% in the high-fat diet
7 vs. crude fat, 5.4% and nitrogen free extracts, 55.3% in the standard diet) and/or the
8 food intake pattern may be related with the significant increase of blood glucose levels.
9 It is necessary to pay attention to background of hyperglycemia at 10 weeks of age in
10 the STZ group.

11 Mice in the HFD group showed obesity, hyperinsulinemia, and hypercholesterolemia,
12 and these changes enhanced over time. Furthermore, the HFD group showed significant
13 increases in lipid accumulation in the liver. Obesity, insulin resistance, and dyslipidemia
14 are major factors that affect the development from hepatic steatosis to NASH (de Alwis
15 and Day, 2008). Insulin resistance is related with overt fat accumulation in ectopic
16 tissues, such as the liver, and increased circulatory free fatty acids, which promote
17 inflammation and endoplasmic reticulum stress, leading to fibrosis (Asrih and
18 Jornayvaz, 2015). It is reported that changes of hepatic lipid profiles, such as increases
19 in acylcarnitine and diacylglycerol levels, were observed in STAM mice toward the
20 fibrosis stage (Saito et al., 2015). Qualitative changes in hepatic lipids are also related

1 with the development from hepatic steatosis to NASH.

2 In conclusion, increases in oxidative stress with hyperglycemia triggered hepatic
3 lesions in STAM mice, and insulin resistance promoted lesion formation with hepatic
4 lipid accumulation, leading to NASH. STAM mice may be a useful model for
5 elucidating the pathogenesis of NASH with diabetes.

6

7

1 **References**

- 2 ASRIH M, JORNAYVAZ FR: Metabolic syndrome and nonalcoholic fatty liver
3 disease: Is insulin resistance the link? *Mol Cell Endocrinol* **418 Pt 1**: 55-65, 2015.
- 4 BUGIANESI E, LEONE N, VANNI E, MARCHESINI G, BRUNELLO F, CARUCCI
5 P, MUSSO A, DE PAOLIS P, CAPUSSOTTI L, SALIZZONI M, RIZZETTO M:
6 Expanding the natural history of nonalcoholic steatohepatitis: from cryptogenic
7 cirrhosis to hepatocellular carcinoma. *Gastroenterology* **123**: 134-140, 2002.
- 8 CLARK JM: The epidemiology of nonalcoholic fatty liver disease in adults. *J Clin*
9 *Gastroenterol* **40 Suppl 1**: S5-10, 2006.
- 10 DAY CP, JAMES OF: Steatohepatitis: a tale of two "hits"? *Gastroenterology* **114**:
11 842-845, 1998.
- 12 DE ALWIS NM, DAY CP: Non-alcoholic fatty liver disease: the mist gradually clears.
13 *J Hepatol* **48 Suppl 1**: S104-112, 2008.
- 14 DOWMAN JK, TOMLINSON JW, NEWSOME PN: Pathogenesis of non-alcoholic
15 fatty liver disease. *QJM* **103**: 71-83, 2010.
- 16 ERTLE J, DECHENE A, SOWA JP, PENNDORF V, HERZER K, KAISER G,
17 SCHLAAK JF, GERKEN G, SYN WK, CANBAY A: Non-alcoholic fatty liver disease
18 progresses to hepatocellular carcinoma in the absence of apparent cirrhosis. *Int J*
19 *Cancer* **128**: 2436-2443, 2011.
- 20 FALCK-YTTER Y, YOUNOSSI ZM, MARCHESINI G, MCCULLOUGH AJ: Clinical
21 features and natural history of nonalcoholic steatosis syndromes. *Semin Liver Dis* **21**:
22 17-26, 2001.
- 23 FUJII M, SHIBAZAKI Y, WAKAMATSU K, HONDA Y, KAWAUCHI Y, SUZUKI K,
24 ARUMUGAM S, WATANABE K, ICHIDA T, ASAKURA H, YONEYAMA H: A
25 murine model for non-alcoholic steatohepatitis showing evidence of association
26 between diabetes and hepatocellular carcinoma. *Med Mol Morphol* **46**: 141-152, 2013.
- 27 GIACCO F, BROWNLEE M: Oxidative stress and diabetic complications. *Circ Res*
28 **107**: 1058-1070, 2010.
- 29 GREENFIELD V, CHEUNG O, SANYAL AJ: Recent advances in nonalcoholic fatty
30 liver disease. *Curr Opin Gastroenterol* **24**: 320-327, 2008.
- 31 ISHII Y, MOTOHASHI Y, MURAMATSU M, KATSUDA Y, MIYAJIMA K, SASASE
32 T, YAMADA T, MATSUI T, KUME S, OHTA T: Female spontaneously diabetic Torii
33 fatty rats develop nonalcoholic steatohepatitis-like hepatic lesions. *World J*
34 *Gastroenterol* **21**: 9067-9078, 2015.
- 35 KUCERA O, CERVINKOVA Z: Experimental models of non-alcoholic fatty liver
36 disease in rats. *World J Gastroenterol* **20**: 8364-8376, 2014.
- 37 PARADIES G, PARADIES V, RUGGIERO FM, PETROSILLO G: Oxidative stress,
38 cardioplipin and mitochondrial dysfunction in nonalcoholic fatty liver disease. *World J*
39 *Gastroenterol* **20**: 14205-14218, 2014.

1 SAITO K, UEBANSO T, MAEKAWA K, ISHIKAWA M, TAGUCHI R, NAMMO T,
2 NISHIMAKI-MOGAMI T, UDAGAWA H, FUJII M, SHIBAZAKI Y, YONEYAMA H,
3 YASUDA K, SAITO Y: Characterization of hepatic lipid profiles in a mouse model
4 with nonalcoholic steatohepatitis and subsequent fibrosis. *Scientific reports* **5**: 12466,
5 2015.

6 TAKAHASHI Y, SOEJIMA Y, FUKUSATO T: Animal models of nonalcoholic fatty
7 liver disease/nonalcoholic steatohepatitis. *World J Gastroenterol* **18**: 2300-2308, 2012.

8 TAKAKURA K, KOIDO S, FUJII M, HASHIGUCHI T, SHIBAZAKI Y,
9 YONEYAMA H, KATAGI H, KAJIHARA M, MISAWA T, HOMMA S, OHKUSA T,
10 TAJIRI H: Characterization of non-alcoholic steatohepatitis-derived hepatocellular
11 carcinoma as a human stratification model in mice. *Anticancer Res* **34**: 4849-4855,
12 2014.

13 YAN LJ: Pathogenesis of chronic hyperglycemia: from reductive stress to oxidative
14 stress. *J Diabetes Res* **2014**: 137919, 2014.

15 YANG J, ZHOU Q, WANG Y, LIU K, ZHANG J: [Effect of high glucose on PKC and
16 MMPs/TIMPs in human mesangial cells]. *Zhong Nan Da Xue Xue Bao Yi Xue Ban* **34**:
17 425-431, 2009.

18 ZELBER-SAGI S, NITZAN-KALUSKI D, HALPERN Z, OREN R: Prevalence of
19 primary non-alcoholic fatty liver disease in a population-based study and its
20 association with biochemical and anthropometric measures. *Liver Int* **26**: 856-863,
21 2006.

22

1 **Figure Legends**

2 **Fig. 1.** Changes in days after treatment in body weight and biochemistry parameters in
3 STAM, HFD, STZ, and Normal groups. (A): Body weight; (B): Glucose; (C): Insulin;
4 (D): Triglyceride (TG); (E): Total cholesterol (TC); (F): Alanine aminotransferase
5 (ALT). Data represent means \pm standard deviation (SD) (n=7-8). *p<0.05, **p<0.01;
6 significantly different from the Normal group.

7

8 **Fig. 2.** Changes in liver weight (A), hepatic triglyceride (TG) (B) and total cholesterol
9 (TC) (C) content, and hepatic tumor necrosis factor (TNF) α (D) and tissue inhibitor of
10 metalloproteinase (TIMP)1 (E) mRNA expression in STAM, HFD, STZ, and Normal
11 groups. Data represent means \pm standard deviation (SD) (n=7-8). *p<0.05,
12 **p<0.01; significantly different from the Normal group.

13

14 **Fig. 3.** Liver histopathology at 5 and 10 weeks of age. (A, E): STAM group; (B, F):
15 HFD group; (C, G): STZ group; (D, H): Normal group. Hematoxylin and eosin (HE)
16 staining. Bar = 100 μ m. Immunohistochemistry of hexanoyl-lysine (HEL) in the liver
17 at 5 weeks of age. (I): STAM group; (J): HFD group; (K) STZ group; (L): Normal
18 group. Bar= 100 μ m.

19

20 **Fig. 4.** Sirius Red staining in the liver at 5, 7 and 10 weeks of age. (A, E and I): STAM
21 group; (B, F and J): HFD group; (C, G and K): STZ group; (D, H and L): Normal
22 group. Bar = 100 μ m.

23

24

1 **Table 1.** Histopathological findings in livers from 4 groups using C57BL6 mice

Animal No.	STAM group																							
	5 weeks of age								7 weeks of age								10 weeks of age							
	1	2	3	4	5	6	7	8	9	10	11	12	13	14	15	MN	17	18	19	20	21	22	23	24
Hepatosteatosi (fatty change)	2+	2+	+	2+	3+	2+	2+	+	2+	+	+	2+	3+	2+	+	2+	3+	2+	3+	+	3+	2+	2+	
Hypertrophy hepatocyte (vacuolation / fatty change)	+	+	±	±	2+	+	+	+	2+	+	2+	2+	2+	2+	2+	2+	3+	2+	3+	+	2+	2+	2+	
Fibrosis	±	±	±	±	+	±	±	±	+	±	±	-	±	±	+	±	+	±	2+	+	±	+	+	

Animal No.	HFD group																							
	5 weeks of age								7 weeks of age								10 weeks of age							
	25	26	27	28	29	30	31	32	33	34	35	36	37	38	39	40	41	42	43	44	45	46	47	48
Hepatosteatosi (fatty change)	+	+	+	+	+	+	±	2+	-	+	+	3+	+	2+	+	+	2+	2+	3+	3+	3+	3+	3+	2+
Hypertrophy hepatocyte (vacuolation / fatty change)	-	±	-	±	-	-	-	±	-	-	±	+	-	±	±	-	+	+	2+	2+	2+	2+	3+	+
Fibrosis	-	-	-	-	-	-	-	-	±	+	-	+	-	-	-	±	-	-	±	±	+	±	-	±

Animal No.	STZ group																							
	5 weeks of age								7 weeks of age								10 weeks of age							
	49	50	51	52	53	54	55	56	57	58	59	60	61	MN	63	64	65	66	67	68	69	70	71	72
Hepatosteatosi (fatty change)	-	-	±	-	±	-	-	-	-	-	-	±	-		±	±	-	±	±	±	±	±	-	±
Hypertrophy hepatocyte (vacuolation / fatty change)	-	-	±	-	-	±	-	-	±	±	±	±	-		±	±	±	±	±	±	+	±	-	±
Fibrosis	±	+	±	-	±	-	+	±	+	±	+	+	±		-	-	-	±	-	±	±	±	+	+

Animal No.	Normal group																							
	5 weeks of age								7 weeks of age								10 weeks of age							
	73	74	75	76	77	78	79	80	81	82	83	84	85	MN	87	88	89	90	91	MN	93	94	95	96
Hepatosteatosi (fatty change)	-	-	-	-	-	-	-	-	-	-	-	-	-		-	-	-	-	-		-	-	-	-
Hypertrophy hepatocyte (vacuolation / fatty change)	-	-	-	-	-	-	-	-	-	-	-	-	-		-	-	-	-	-		-	-	-	-
Fibrosis	-	-	-	-	-	-	-	-	-	-	-	±	-		-	-	-	-	-		-	-	-	-

2

3 Grade: ± Very slight, + Slight, 2+ Moderate, 3+ Severe. MN: missing number.

4 Fibrosis was evaluated using Sirius red staining.

5

6

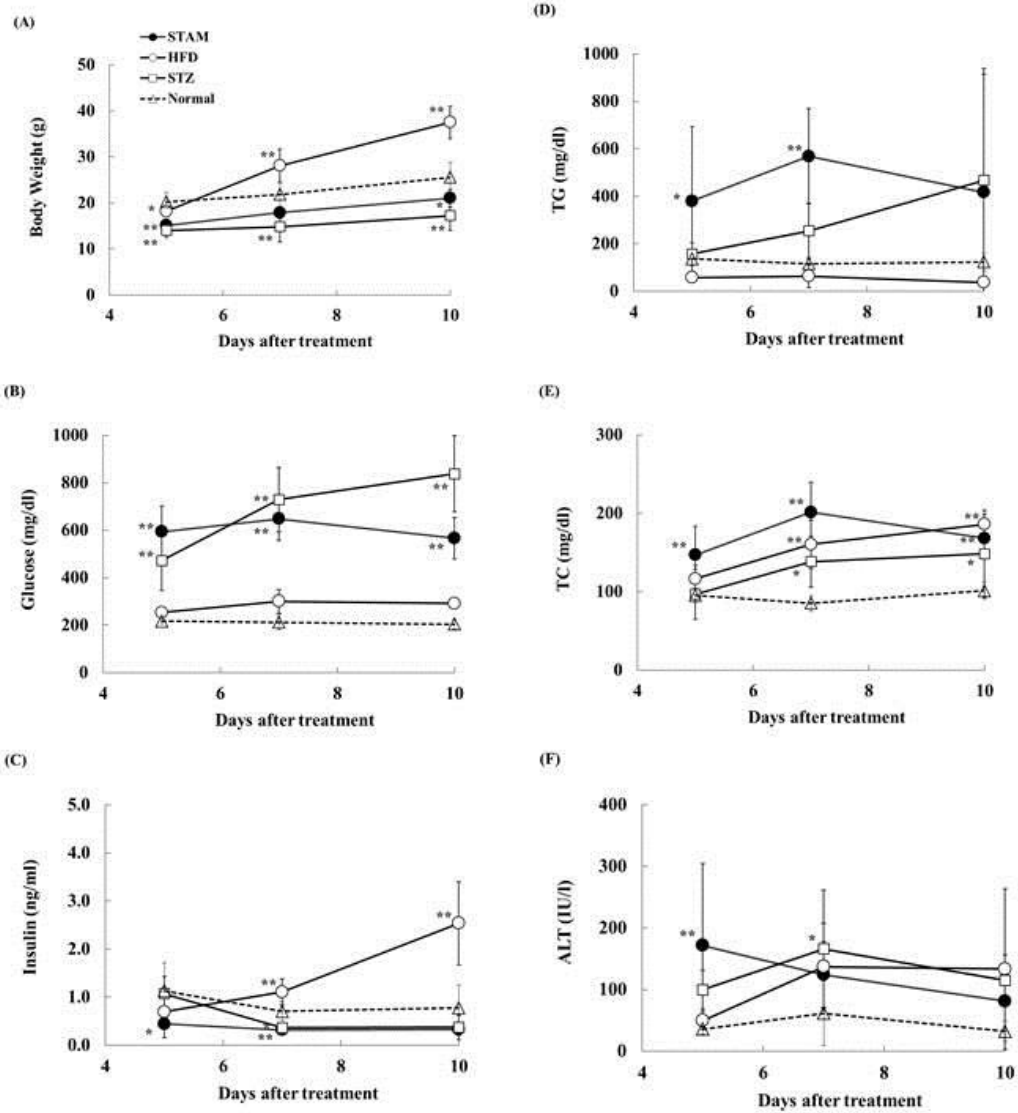


Fig. 1

1
2

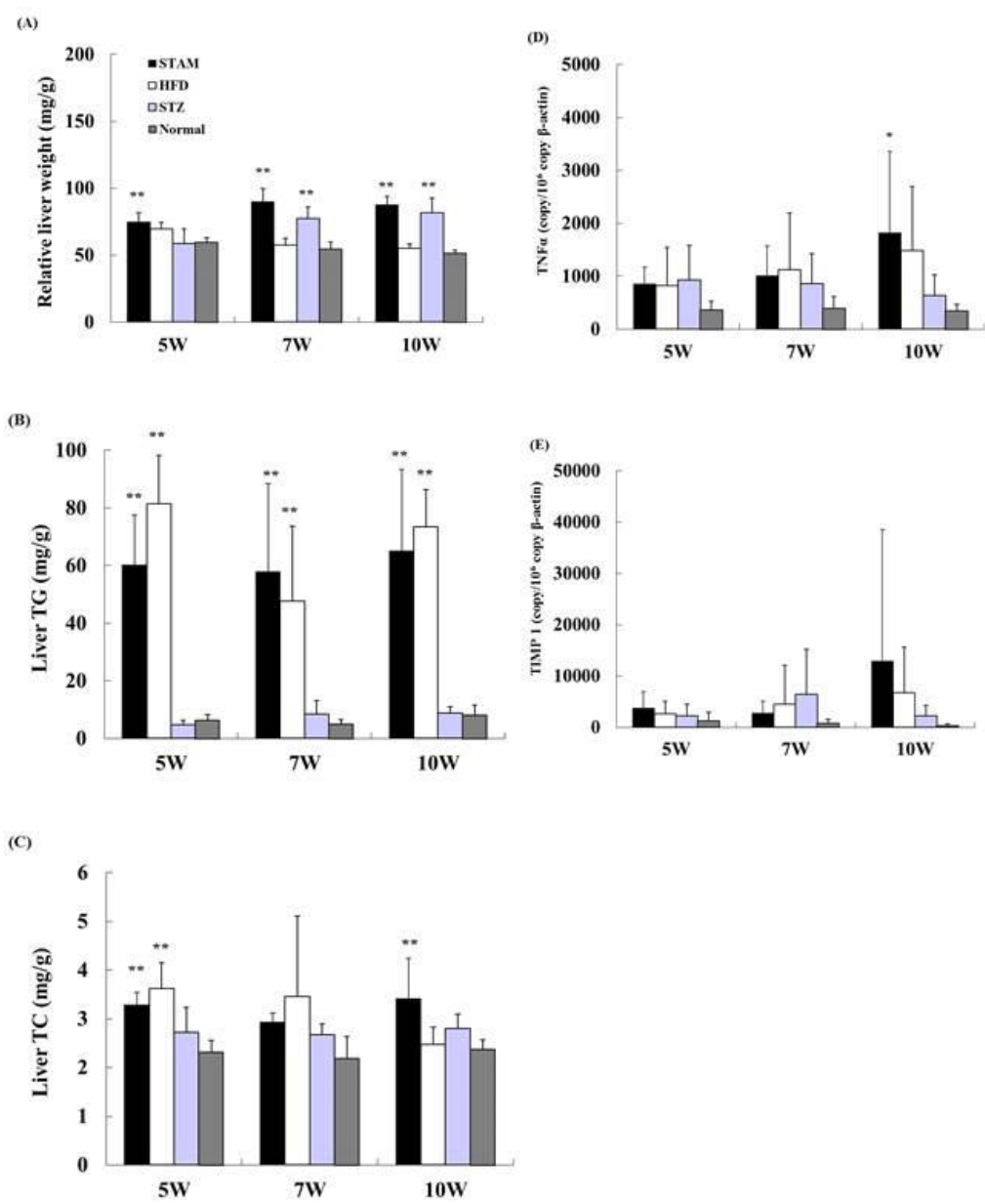


Fig. 2

1
2

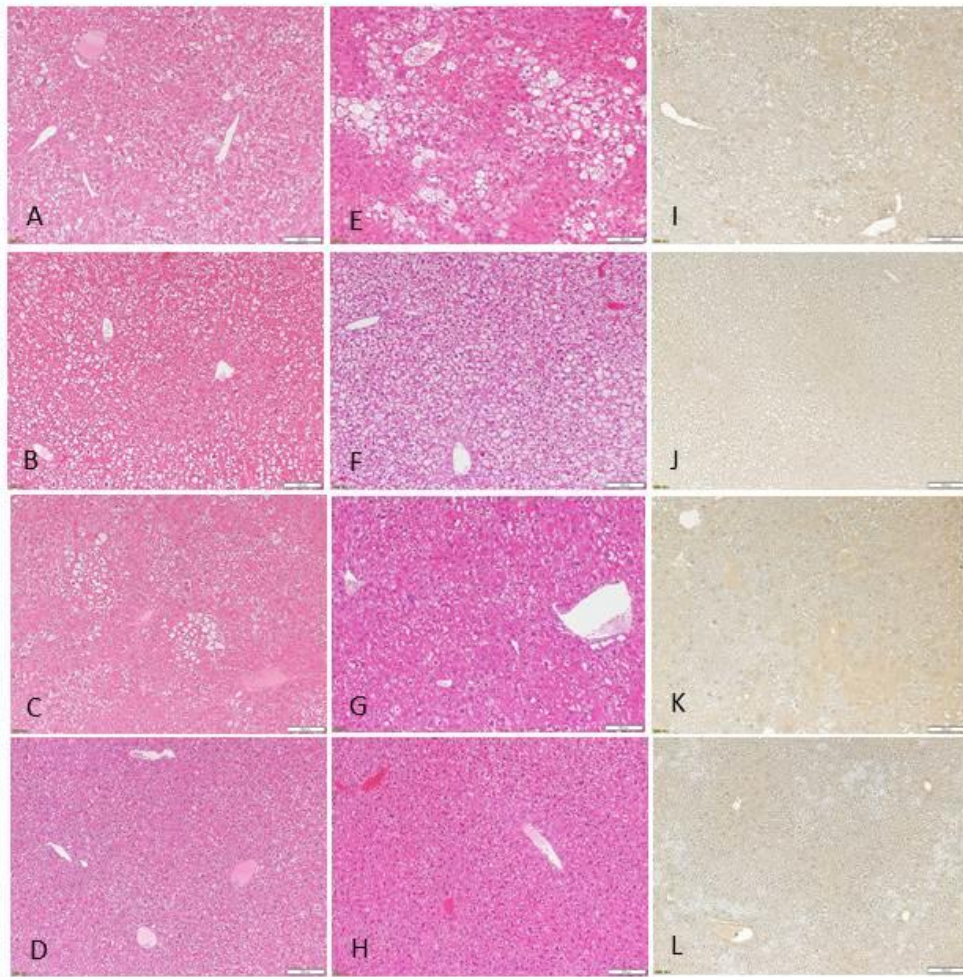


Fig. 3

1
2

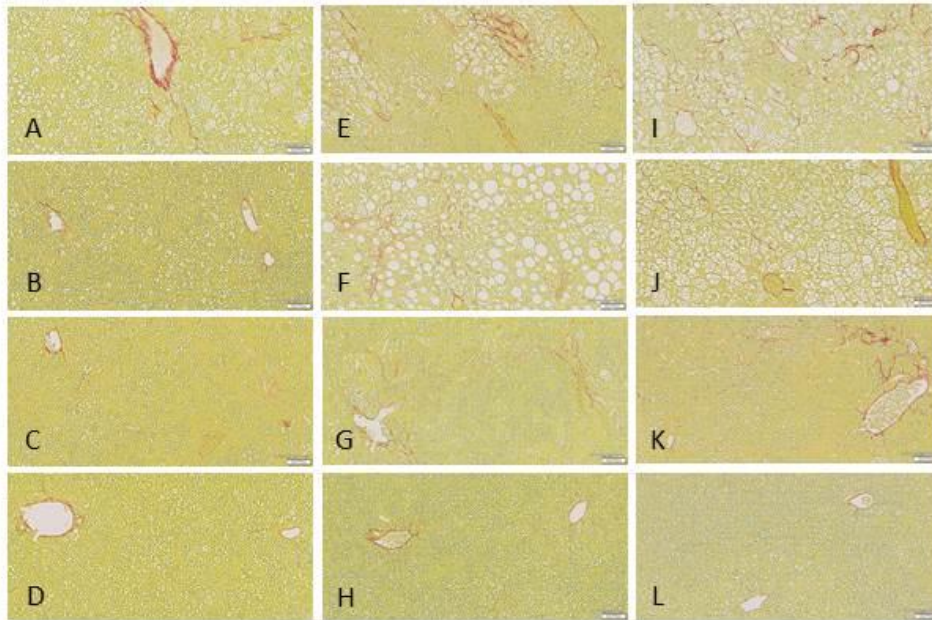


Fig. 4